NASA Technical Memorandum 103795

Evaluation and Ranking of Candidate Ceramic Wafer Engine Seal Materials

Bruce M. Steinetz
Lewis Research Center
Cleveland, Ohio

May 1991

NASA

EVALUATION AND RANKING OF CANDIDATE CERAMIC WAFER ENGINE SEAL MATERIALS

Bruce M. Steinetz
National Aeronautics and Space Administration
Lewis Research Center
Cleveland, Ohio 44135

SUMMARY

Modern engineered ceramics offer high temperature capabilities not found in even the best superalloy metals. The high temperature properties of several selected ceramics including aluminum oxide, silicon carbide and silicon nitride are reviewed as they apply to hypersonic engine seal design. A ranking procedure is employed to objectively differentiate amongst four different monolithic ceramic materials considered, including: a cold-pressed and sintered aluminum oxide; a sintered alpha-phase silicon carbide; a hot-isostatically pressed silicon nitride; and a cold-pressed and sintered silicon nitride. This procedure is used to narrow the wide range of potential ceramics considered to an acceptable number for future detailed and costly analyses and tests. The materials are numerically scored according to their high temperature flexural strength; high temperature thermal conductivity (providing a measure of the amount of active cooling required); resistance to crack growth; resistance to high heating rates; fracture toughness; Weibull modulus; and finally according to their resistance to leakage flow, where materials having coefficients of thermal expansion closely matching the engine panel material resist leakage flow best. The cold-pressed and sintered material (Kyocera SN-251) ranked the highest in the overall ranking especially when implemented in engine panels made of low expansion rate materials being considered for the engine, including Incoloy and titanium alloys.

INTRODUCTION

NASA Lewis is developing several seal concepts to be used to seal the many feet of sliding interfaces between articulating panels and stationary engine splitter walls of advanced hypersonic engines. An example of one these seals is the ceramic wafer seal shown in figure 1 installed in a close tolerance seal channel machined in the movable horizontal engine panel. The goal of the seal is to prevent the superheated, pressurized engine gases flowing beneath the panel from escaping behind the seal to backside engine cavities. As has been described elsewhere (refs. 1 to 4), the seal is composed of a series of thin ceramic wafers preloaded from behind using a series of Inconel metal bellows to accommodate the significant adjacent wall distortions, where distortions can be as large as 0.15 in. in only an 18 in. span.

Selecting the best materials for the panel-edge seals, the seal designer is faced with difficult choices to make. The seal must be strong and light-weight, must survive the thermally aggressive environment, must resist hydrogen embrittlement and oxidation, and must resist chipping and abrasion damage while sliding against the adjacent engine panels.

While investigating materials suitable for the high temperature service conditions of the wafer seal, four groups of materials were considered. These materials included carbon-carbon composites, refractory metals, superalloy metals, and engineered ceramics.

Carbon-carbon composites exhibit very high operating temperatures (up to 3000 °F), and have very high strength-to-weight ratios but are rapidly consumed by oxidation. Refractory metals such as Columbium have high operating temperatures ($\geq$2500 °F) but are heavy and also oxidize rapidly. Both of these materials were rejected as wafer materials because of their poor oxidation performance and the need for failure-prone protective coatings.

Selected superalloy metals are resistant to oxidation and hydrogen embrittlement but have limited maximum operating temperatures (<1800 °F), requiring considerable cooling. Because of their high weight-density, superalloy materials result in heavy seal designs.

Engineered ceramics have been advanced over the past decade and show promise of meeting the challenging seal design criteria. These ceramics can operate at temperatures 800 °F above superalloy materials, and have high specific strength (e.g., strength divided by weight-density) at temperatures exceeding 2200 °F. Ceramic materials are resistant to abrasion due to their high hardness. However, ceramics are brittle by nature and must be properly selected and applied.

Several types of ceramics including aluminum oxides, silicon carbides and silicon nitrides have been improved through improved processing techniques that minimize volume and surface fracture initiation sites. Techniques employed include reducing grain size, maintaining very high purity, using improved sintering agents, and following strict quality control. Making tradeoffs between these types of ceramics is sometimes difficult since material property data are difficult to assemble because only recently are standard tests being performed over the full temperature range. In assembling property data, one must be careful in that some manufactures will quote material properties (e.g., fracture toughness and flexural strength) using test methods which are known to give overly optimistic results.

Once the material properties are assembled, a means for objectively selecting between competing materials is required to select the best material prior to final detailed and costly design analyses and tests.

The objectives of this study are to investigate and compare a range of thermal, structural, and chemical properties of a selected number of monolithic engineered ceramics and objectively rank the relative performance of these materials as they apply to the design of hypersonic engine seals.

MATERIAL REQUIREMENTS

A seal material is required to fulfill several important criteria to be considered viable for hypersonic engine seal design. Listed below are some of these criteria:

(1) Operate hot at temperatures $\geq$2000 °F.

(2) Have low weight density to minimize seal and subsystem weight to help meet vehicle weight goals and enable the single-stage-to-orbit mission.

(3) Have good thermal properties such as high thermal conductivity and high thermal diffusivity to operate in the high heating rates (up to 1500 Btu/ft^2-s) of hypersonic engines, requiring minimal coolant.

(4) Have high strength to sustain the engine thermal and structural loads. Have an acceptable variability of strength properties to provide adequate component reliability for the several thousand of seal elements required in an engine.

(5) Have high fracture toughness to resist chipping and fracture during sliding operation.

(6) Resist chemical attack including oxidation and hydrogen embrittlement at the high engine gas temperatures.

(7) Resist thermal shock during either the extreme heating or cooling transients anticipated during engine operation.

(8) Resist leakage flow between wafers by having thermal expansion rates approximating those of the engine panels.

RESULTS AND DISCUSSION

Material Property Comparisons

Three types of monolithic ceramics were considered in this investigation including aluminum oxide, silicon carbide and silicon nitride. The aluminum oxide was a cold-pressed and sintered Greenleaf[1] Technical Ceramics, designated 99 percent-pure grade. The silicon carbide considered was a sintered-alpha material from Carborundum Co., designated Hexoloy SA grade. The sintered-alpha material was chosen because of its high thermal conductivity. This silicon carbide has a conductivity 60 percent higher than high temperature superalloy metals even at high temperature. Three silicon nitrides were considered: two cold pressed and sintered versions from Kyocera Ceramic (designated SN-220 and SN-251); and a reaction-bonded silicon nitride from Garrett Ceramic Components Div., designated GN-10. In subsequent sections of this study, key material properties of these ceramics are compared and a procedure for selecting a material having the optimum balance of material properties is developed.

Operating Temperature

Listed in table I are the operating temperatures of ceramics considered in this investigation along with room and high temperature properties compiled from a variety of sources. Of the three types of ceramics considered, aluminum oxide has the highest operating temperature in air environments. Aluminum oxide being an oxide ceramic is very stable to temperatures up to 3000 °F. Silicon carbide maintains useful properties up to 2300 to 2500 °F and silicon nitride ceramics maintain useful properties from 1650 to 2500 °F depending on the type of ceramics considered. The SN-220 material has a 1650 °F upper temperature limit and hence is not further considered in this investigation.

---

[1] Note: Mention of manufacturers is made only for reference purposes and does not constitute a product endorsement by NASA or the U.S. Government.

Flexural Strength

Average flexural strengths for aluminum oxide, silicon carbide and the silicon nitrides meeting the 2000 °F operating temperature requirement are plotted in figure 2 at room temperature and 2200 °F. Three- and four-point bend tests data are typically published in the literature instead of the tension test data because of the relative simplicity and cost savings of specimen manufacture and test (ref. 5). In the four-point bend test, a flat specimen is supported and loaded at two points each (ref. 5) loading the center gage section in a uniform bending stress. The four-point bend tests result in more representative strength values because of the larger volume of material that is fully stressed between the two center loading pins. Ceramic specimens following statistical failure behavior are more likely to fail as the specimen volume is increased. The stressed-volume of the typical four-point bend test specimen is very close to the ceramic wafers, therefore the flexural strengths in table I are considered representative of the expected strengths in the wafer elements.

The Garrett GN-10 and the Kyocera SN-251 silicon nitride materials have the highest flexural strengths of all of the ceramics considered at room temperature and at 2200 °F. High strength is required to sustain the thermal and mechanical stresses induced in the ceramic wafers. In reference 4, a thermal structural analysis was conducted for the silicon carbide material under the Mach 10 engine heating rates. This study concluded that the steady state stresses were 24 ksi, and were below the average tensile strength of 35 ksi (ref. 6) for silicon carbide at 2200 °F. The limited safety margin, the potential for higher transient thermal stresses, and the dispersion associated with ceramic strength data, however, indicated that alternative materials should be considered.

Fracture Toughness

Another important property of ceramic materials is the fracture toughness, K_{1C} (ref. 5). A material's K_{1C} is a measure of stress intensity at the tip of a crack that will cause a crack to propagate and lead to failure. Therefore the higher the material's fracture toughness the more difficult it is for a crack to propagate. The fracture toughnesses of the ceramic materials considered are plotted in figure 3.

The fracture toughness of silicon nitride is again the highest as a material class. The SN-251 material has the highest fracture toughness of 6.3 ksi$\sqrt{\text{in.}}$ The high fracture toughness combined with the relatively low elastic modulus makes this material more resistant to fracture relative to the other ceramic considered.

Weibull Modulus

Ceramic materials are brittle by nature and furthermore can have a significant scatter in their strength data. Reference 5 demonstrates the typical scatter in strength for ceramics relative to high temperature superalloy metals and shows that the variability can be twice that of metals. Ceramic material strength data follows a Weibull distribution, where strengths do not fall evenly around a median.

One measure of the size of the strength data-scatter is given by the Weibull modulus, often referred to in the literature by "m." The Weibull modulus is the slope of the probability of failure versus the material's strength with the data

plotted on log-log coordinates. A higher Weibull modulus indicates a relatively narrow scatter of data, and subject to a certain reliability allows one to more closely predict the likelihood of component survivability subject to given loading conditions. Weibull modulus can also be viewed as a measure of the flaw size distribution. For a detailed discussion of Weibull statistics one may refer to (ref. 7). The Weibull moduli for the four ceramic materials are plotted in figure 4 at room temperature in an air environment. The SN-251 silicon nitride has the highest modulus of 17.

Thermal Properties

The intense heating rates and the high gas temperatures found in advanced hypersonic engines require materials that can withstand high thermal transients and require minimal active coolant. A material's thermal diffusivity, which is the ratio of conductivity to the material's density and heat capacity is a measure of the rate at which the heat applied to the seal's exposed surface is diffused through the body. As can be seen by figure 1, a narrow band of the seal wafer surface is subjected to the high heat flux. Enhancing the rate at which the heat applied to the exposed surface diffuses through the wafer and into adjacent cooled engine surfaces lowers the thermal stresses at the material's surface. The thermal loads dominate the structural loads so high diffusivity is key.

Thermal diffusivity is plotted in figure 5 at room temperature and at 2200 °F. At both temperatures, the sintered-alpha silicon carbide has the highest thermal diffusivity because of its high thermal conductivity. It is noted from table I that the thermal conductivity for all of the ceramics drops with increasing temperature resulting in lower thermal diffusivity at temperature. It is noted from figure 5 that the differences in thermal diffusivity at higher temperatures is considerably less than at low temperatures.

Under steady state heat transfer conditions, the material's thermal conductivity plays a key role. The high (>5000 °F) gas temperatures expected in the engine requires that some form of active cooling be used. In the analysis conducted in reference 4, purge cooling the seal with ambient temperature (70 °F) helium pressurized at 15 psi above engine chamber pressure combined with thermal conduction into adjacent panels were sufficient to maintain maximum seal temperatures below the 2500 °F limit of silicon carbide. Materials with lower thermal conductivity at temperature would require proportionately more coolant.

Thermal Shock Resistance of Brittle Materials

Common to everyday experience with glass, brittle materials are susceptible in varying degrees to damage due to thermal shock. The fundamental mechanism of thermal shock is that an applied temperature difference causes thermal strain in materials with a finite thermal expansion rate, which can lead to high local stresses and subsequent fracture. If either the applied temperature or heating rate are high enough, stresses will result that upon encountering a flaw will lead to fracture or degradation of mechanical strength. Hasselman (ref. 8) has recommended several parameters that provide a measure of the brittle material's resistance to thermal shock damage. The two parameters (refs. 5 and 8) that apply to the heating conditions of hypersonic engine seals are given below. The resistance parameter R' in equation (1) is

proportional to the sudden temperature difference required to cause an initiated crack to continue propagating.

$$R' = \left(\frac{\gamma}{\alpha^2 E}\right) \qquad (1)$$

$$\gamma = \frac{K_{1C}^2(1 - \nu^2)}{2E}$$

R' is calculated using room temperature properties since these are typically known. In these relations, E is the elastic modulus; γ is the fracture energy; K_{1C} is the material's fracture toughness; α is the material's coefficient of thermal expansion; and ν is Poisson's ratio.

The R' parameter is calculated for all of the ceramic materials and are shown in figure 6. The Kyocera SN-251 material had the highest calculated resistance due to its excellent fracture toughness, low coefficient of thermal expansion and relatively low modulus.

The resistance parameter R'' in equation (2) is proportional to the maximum allowable rate of surface heating.

$$R'' = \frac{\sigma(1 - \nu)\alpha_{TH}}{\alpha E} \qquad (2)$$

R'' is conservatively calculated using the material's high temperature (2200 °F) properties where the strength σ and thermal diffusivity α_{TH} are lowest. (Note: The tabulated flexural strength was used in place of the tensile strength in eq. (2).)

The R'' parameters are calculated for each of the ceramic materials and are shown graphically in figure 7. The Garrett GN-10 material exhibits the highest value due to the material's excellent flexural strength at 2200 °F. Though the silicon carbide material is not as strong as the SN-251 material, silicon carbide's high thermal diffusivity can quickly diffuse the heat through the seal wafer and gives this material a relatively high R'' resistance.

Thermal Expansion Effects on Seal Leakage

In successfully applying ceramics to advanced heat engine applications, one must account for the potential impact of the difference in the coefficient of thermal expansion (CTE) of the ceramic and the surrounding materials. Typically CTE mismatches pose problems since one is attempting to bond the ceramic to relatively high expansion rate materials. Fortunately in the ceramic wafer seal application the wafers move in the seal channel and require no ceramic-to-metal joining. However the difference in CTEs enters the design process in a second subtle way. As the engine heats up, the panel and the seal grow according to their respective thermal expansion rates, where the axial direction is of greatest concern. If the panel has a substantially higher CTE than that of the ceramic wafers, narrow inter-wafer gaps can open up between the wafers. If these inter-wafer gaps are too large, the seal will leak

unacceptably. Earlier in this work (also ref. 3), a model was developed to predict the leakage flow per unit length ($\dot{m}/L$) past the seal, as a function of: the difference in the squares of the upstream (P_s) and downstream (P_o) pressures; the effective leakage gaps at the top and nose seal contacts ($h_{1,v}$, $h_{2,v}$); the seal contact dimensions (H_1, H_2); the inter-panel gap width (g); the number of wafer interfaces (N); and the gas properties (μ = gas viscosity; R = universal gas constant; and T = gas temperature):

$$\dot{m}/L = \frac{\left(P_s^2 - P_o^2\right)}{24\mu RT}\left(\frac{h_{1,v}^3}{H_1} + \frac{h_{2,v}^3}{H_2} + \frac{Ngh_{CTE}^3}{LH_2}\right) \tag{3}$$

In this equation the effective inter-wafer spacing is found from:

$$h_{CTE} = (\alpha_{engine\ \ panel} - \alpha_{wafers})\frac{L\Delta T}{N} \tag{4}$$

where N is the number of wafer interfaces (e.g., the number of wafers minus 1), L is the seal length and ΔT is the temperature rise.

From equations (3) and (4) it is clear that the leakage is dependent on difference in the expansion rates of the wafer seal and the engine panel to the cubed power. Hence this simple material parameter can considerably effect the leakage rates if the difference in the wafer and the engine panel CTEs is too great.

Rearranging equation (3) one can formulate a leakage flow resistance parameter where leakage flow resistance is defined as:

$$R_F = \frac{P_s^2 - P_o^2}{\dot{m}/L} \tag{5}$$

specifically:

$$R_F = \frac{24\mu RT}{\left(\frac{h_{1,v}^3}{H_1} + \frac{h_{2,v}^3}{H_2} + \frac{Ngh_{CTE}^3}{LH_2}\right)} \tag{6}$$

Using a tentative leakage flow limit in equation (5) combined with the maximum anticipated pressure drop of 100 psi across the seal, one can calculate a minimum flow resistance, R_F for anticipated engine seal material and engine panel material combinations. As described in reference 3, the tentative leakage flow limit established for the panel edge seals was 0.004 lb/s-ft of seal length. Substituting these values into equation (5) results in a minimum flow resistance of:

$$R_{F,min} = 6.7 \times 10^{10} \frac{lb\ s}{ft^3}$$

Leakage flow resistances were calculated for two candidate high temperature superalloy engine materials at a temperature of 1400 °F. Final engine material selection has not yet been made, so two materials with widely different expansion rates were considered for these calculations to cover the range of possible expansion rates. For the purposes of this example, it was assumed that the gas temperature, the wafer temperature and the engine panel temperature were all equal to 1400 °F. It is recognized that engine gas temperature and hence the seal temperature can be substantially higher than this. If they were higher, however, the calculated resistances would be even higher than that calculated herein.

The first superalloy material considered is a relatively high expansion alloy HS-188. HS-188 is a cobalt-based alloy that has excellent high temperature ultimate and creep strengths, good oxidation resistance, and is resistant to hydrogen embrittlement (ref. 9). From an expansion-rate point of view, HS-188 (CTE = 9.0×10^{-6} in./in. °F at 1400 °F) is representative of the high CTE materials under consideration for the hypersonic engine panels.

The second engine panel material considered was Incoloy 909, (ref. 10). Incoloy 909 is a nickel-based superalloy but is formulated without chromium to specifically have low expansion rates. The absence of the chromium limits its high temperature oxidation resistance to temperatures below 1200 °F. Above these temperatures some form of oxidation resistant coating is required and the strength is somewhat limited. Incoloy 909 is also resistant to hydrogen attack. From an expansion-rate point of view Incoloy 909 (CTE = 6.1×10^{-6} in./in. °F at 1400 °F) is representative of the low CTE materials under consideration for the engine panels, including titanium alloys.

Flow resistances for wafer seals made of each of the four candidate ceramics "mounted" in each of these engine materials were calculated and are graphically shown in figure 8. The dashed horizontal line in the figure is the minimum flow resistance calculated using equation (6) above. High expansion rate aluminum oxide meets the flow resistance parameter for both engine materials. Aluminum oxide wafers 0.125 in. thick were tested in reference 3 in an Inconel X-750 test fixture simulating the engine. (Note: For reference Inconel X-750 and HS-188 have nearly identical thermal expansion rates, so the difference in wafer and panel CTEs and hence leakage flow resistances would be similar). The leakage flow rates were below the tentative leakage limit at 100 psi at 1350 °F.

The low expansion rate silicon carbide and silicon nitride ceramics fell below the minimum resistance by 18 and 23 percent respectively when "mounted" in the high expansion rate HS-188 simulated engine material. However, the flow resistances of each of these ceramics exceeded the minimum resistance by considerable margins when "mounted" in the low expansion rate Incoloy 909 engine material.

Final selection of the engine material will not be made for some time in the future. If a high expansion rate material is used for the engine panels, there are several kinematic approaches that can be considered to overcome the differential axial thermal expansion between the ceramic and the engine panels. One approach invented by the author is depicted in figure 9. In this approach, the wafer pieces

are manufactured in wedge shaped pieces and are loaded in the seal channel in an alternating fashion. The wafers are designed with appropriate dimensions so that as the engine panel and seal heat up, the bellows pressing against the backsides of the wafers convert lateral motion into axial growth of the wafer stack to accommodate the thermal expansion mismatch. The wafers are designed with "truncated" tips so that as the expansion occurs the pin-hole size leakage paths existing at room temperature seal at the design condition. The wafer wedge angles and solid film lubricants are selected such that the friction coefficients between the wafers is less than the tangent of the wedge angle so that the wedges disengage upon cool down.

Friction Coefficients

Another parameter requiring consideration in sliding seal design are friction coefficients and seal wear. For the wafer seal design there are two classes of sliding seal contacts: ceramic-to-metal sliding as the seal is slid against the sidewall and actuated in its seal channel; and ceramic-to-ceramic sliding between the adjacent wafers as the wafers move relative to one another to accommodate engine sidewall distortions.

Unlike long-life face-seals, the seal sliding speeds are relatively slow. Using the high temperature pin-on-disk tribometer at NASA Lewis (ref. 11), friction coefficients for low-speed sliding contacts were generated at room and elevated temperatures for the general classes of ceramics considered herein. In the tribometer shown in figure 10, a hemispherically shaped pin is held in sliding contact against the face of a spinning or oscillating disk depending on test conditions. The friction coefficients are determined as the ratio of the measured tangential and applied normal loads.

Ceramic friction coefficients were measured at room temperature and at 1650 °F sliding against either Inconel X-750, simulating the engine sidewall material, or against themselves. Maximum contact stresses were between 61 to 75 ksi for the ceramic-to-ceramic contacts and between 54 to 58 ksi for the ceramic-to-metal contacts.

The ceramic-to-ceramic friction coefficients were all quite high (see table II) ranging from 0.5 to 1.0. Advanced high temperature solid film lubricant approaches (ref. 12) are under development to reduce these friction coefficients to acceptable levels (e.g., ≈0.4) to minimize the chances of binding between adjacent wafers. The ceramic-to-metal friction coefficients were high at room temperature but decreased to 0.3 to 0.35 at high temperature where the metal oxide begins to act as a solid film lubricant.

Environmental Effects

Seal materials considered for these hydrogen-fueled hypersonic engines must resist hot hydrogen and oxidation attack. Hydrogen embrittlement at temperature is a condition in which the small energetic H_2 molecule weakens the grain boundaries and degrades the parent material strength. Perhaps one of the most dramatic forms of hydrogen embrittlement is when H_2 diffuses into a material and combines with free carbon. In this case methane is formed and if oxygen is present the mixture can combust locally within the material.

Limited testing has been conducted to assess the effects of hot hydrogen on these engineered ceramics. Strength tests and thermodynamic analyses recently performed at NASA Lewis have shed considerable light on this important issue. In this investigation (ref. 13) the effects of moist hydrogen on the flexural strengths of silicon nitride, silicon carbide, and aluminum oxide amongst other ceramics were assessed from room temperature up to 2550 °F. As is indicated in table I taken from reference 13, the hydrogen had little if any effect on the strength of each of the three types of ceramics. The noted loss in strength is no different than the strength loss simply due to the higher operating temperature.

The metal bellows and the seal backing strip which form the lateral preload system of the seal were both made of Inconel 718. This material shown only minor hydrogen weakening (ref. 9) and is used extensively on the hydrogen-oxygen Space Shuttle Main Engine.

Oxidation. - Aluminum oxide being an oxide is typically stable in an oxygen or air environment at high temperature (ref. 5). Therefore no variation in properties are anticipated due to the presence of oxygen.

The carbide and nitride classes of ceramic typically react with oxygen. The reaction with silicon, however, quickly forms a protective SiO_2 surface layer (ref. 5) under partial pressures of oxygen of interest. This process is known as passive oxidation and under these conditions, further oxidation will be slow and be controlled by oxygen diffusion though the SiO_2 layer. Oxidation has been noted to reduce strength in Si_3N_4 at high temperatures but requires somewhat longer times than the few hundred hours of life for these seals. Conservatively, however, one should conduct tests in a simulated environment to make the final assessment.

The Inconel 718 material used for the bellows preload system and seal backing strip have good mechanical properties in air environments and temperatures up to 1300 °F, (ref. 14).

Seal Weight

Because of the significant lengths (≈40 ft) of seal required per engine, designers must incorporate minimum weight materials and design concepts. Ceramics offer significantly lower weight densities 1/3 to 1/2 than those of superalloy metals, resulting in a low weight seal design.

The seal weights were determined by measuring the weight per linear foot of the 0.5-in. seal wafers, 12 Inconel bellows and the thin 0.030 in. seal backing strip between the bellows and the wafers (fig. 1). The dry seal weights (e.g., without seal coolant) for all of the various ceramics considered are tabulated in table I. The seal weights varied from 0.61 lb/ft for silicon carbide and one silicon nitride to 0.70 lb/ft for the aluminum oxide. For comparison purposes, the weight of a Inconel wafer seal (0.5-in. square) would be 1.12 lb/ft, 60 percent higher than the ceramic designs.

Observed Performance of SiC and Al_2O_3

To establish an understanding of the fabrication processes involved with high temperature ceramics and to measure leakage rates of the ceramic wafer seal concept,

wafer specimens were made from the Greenleaf cold-pressed and sintered aluminum oxide, and the Carborundum sintered-alpha silicon carbide. Considerable leakage testing has already shown the successful leakage performance of the aluminum oxide wafer seal. Shown in figure 11(a) are some aluminum oxide wafers after about 20 hr of high temperature (up to 1350 °F) and high pressure (up to 100 psi) testing. The wafers show only a slight change in color. Some of the blackening could be a result of being in contact with the Inconel X-750 rig that formed a greenish-black passivating oxide layer during the tests. There was no observed chipping of the wafer corners or sealing surfaces.

The silicon carbide wafers are shown in figure 11(b) after a single test at room temperature at pressures up to 100 psi. Some of the wafer corners chipped or spalled-off during the tests. This result was a surprise since the wafers were subjected to relatively benign conditions. The leakage rates measured for these wafers were considerably higher than those measured for the aluminum oxide wafers. The wafer corner chipping problem allowed a considerable amount of air to leak past the seal.

Radiography of the seal wafers performed after the tests revealed inclusions and impurities in the wafers with some found near the corners. Some of the chips seemed to originate from minute chips left over form the wafer manufacturing process. These minute chips and material imperfections (e.g., crack initiation sites) combined with silicon carbide's low fracture toughness are believed to have led to the corner fracturing.

It is clear from this experience that silicon carbide's poor fracture toughness limits this supplier's silicon carbide as a seal material for the hypersonic engines. It is noted from this experience that for this high conductivity sintered-alpha silicon carbide to be further pursued as a wafer material, methods of producing near-inclusion-free, fracture tough wafers must be matured. It is noted that considerable material improvements are underway at various manufacturers to overcome the noted limitations.

Seal Material Ranking

The key mechanical, thermal, and leakage performance parameters discussed above were combined into an overall seal material ranking parameter to give an objective relative ranking of the materials. The material's thermal properties are well represented in the ranking parameter because of the severe thermal environment in which the seals must operate. In this study, each of the performance parameters were designed such that high values indicated good performance. Because each of the parameters play a near equal role in determining the materials performance in the final application, the overall material ranking parameter R_M was calculated as a simple sum of the elemental performance parameters according to the following equation:

$$R_M = \frac{\sigma_{flex,2200}}{\rho} + R' + R'' + K_{2200} + R_F + K_{1C} + m_{Weibull} \qquad (7)$$

where:

$\frac{\sigma_{flex,2200}}{\rho}$ = 2200 F Specific flexural strength

R' , R'' = Thermal resistance parameters

K_{2200} = 2200 F Thermal conductivity

R_F = Flow resistance parameter

K_{1C} = 70 F Fracture toughness

$m_{Weibull}$ = 70 F Weibull modulus

In this expression, the elemental parameters are all of different order of magnitudes. To allow each parameter to enter the basis with equal weight, the elemental parameters had to be normalized before summing them. The elemental parameters were normalized with respect to the values of the elemental parameter for the strongest ceramic considered, GN-10. It is also noted that the lead term was the material's specific strength (e.g., strength-to-density ratio) which emphasizes the need for strong and light-weight seal structures. The material friction coefficients were not included in the ranking parameter because their nearly equal magnitudes would not help discriminate between the materials.

Plotted in figure 12 are the results of these studies. Since the flow resistance parameter depends on the engine panel material in which the seal is mounted, two ranking parameters are given for each of the ceramics, as noted. The study shows that the silicon nitride material as a material class outperforms the aluminum oxide and the silicon carbide for this seal application. This assumes however that the seal is mounted in an engine material with a relatively low expansion material such as Incoloy 909 or a titanium alloy. If the seal is to be mounted in the high expansion rate material then the noted shortfall in seal flow resistance can be addressed through methods discussed. As shown in figure 12, the high fracture toughness, high Weibull modulus silicon nitride SN-251 had the highest overall ranking. Repeating the calculations of R_M using the toughest material (e.g., SN-251) as the normalizing basis as opposed to the strongest material (e.g., GN-10) resulted in the same highest ranking material, SN-251.

A designer choosing between the two silicon nitrides for the final engine application would have to consider such things as: wafer reliability; long term material properties; detailed thermal-stress analyses, as conducted in reference 4; material transient heating response; and material cost and availability.

Furthermore, ceramic materials are continuously evolving and improving. Hence over a typical engine design cycle, designers must monitor material developments to optimize the end product. Also, working closely with the material manufacturers, the seal designer and manufacturers may be able to slightly change the material chemistry or sintering aids to improve material performance for the final specific application.

SUMMARY AND CONCLUSIONS

An overview has been presented of the key mechanical, thermal, and chemical properties of several engineered ceramics as they apply to the design of high temperature seals for advanced hypersonic engines, including those for the National Aerospace Plane (NASP). Ceramics offer high operating temperatures, excellent strength at temperature, and low weight density (1/3 to 1/2 that of superalloy metals) resulting in a low weight seal design. The ceramic materials considered resist H_2 attack and have limited oxidation at high temperature.

The ceramic materials reviewed included: a high purity cold-pressed and sintered aluminum oxide (Greenleaf Technical Ceramics, 99 percent grade); a sintered-alpha silicon carbide (Carborundum Co., SA); a hot-isostatically-pressed silicon nitride (Garrett Ceramic Components, GN-10); and a competing cold-pressed and sintered silicon nitride (Kyocera Engineering Ceramics, SN-251).

The key mechanical properties important to engine seal design were examined and compared. The four-point flexural strengths of each of these materials were reviewed at room temperature and 2200 °F, and in order of increasing strength were aluminum oxide, silicon carbide, SN-251 and GN-10 silicon nitrides. Room temperature fracture toughnesses, a measure of the materials resistance to crack growth, were reviewed and in order of increasing toughness included aluminum oxide, silicon carbide, GN-10 and SN-251 silicon nitrides. Weibull moduli which indicate the amount of data scatter in material strength were reviewed and in order of decreasing data scatter include silicon carbide, aluminum oxide, and GN-10 and SN-251 silicon nitrides.

Because of the severe thermal environment of advanced hypersonic engines, good thermal properties such and thermal diffusivity and thermal conductivity are key for good thermal performance of the seal. Thermal diffusivity, a measure of the rate at which the seal material can diffuse sudden thermal transients, were presented for room temperature and 2200 °F and in increasing order included aluminum oxide, GN-10 and SN-251 silicon nitrides, and silicon carbide. The thermal conductivity, a measure of amount of active coolant required to maintain seal temperatures, follows the same order.

Two thermal shock resistance parameters were examined for relative ranking amongst the ceramic materials. The first parameter measured the ceramic's resistance to crack growth and is proportional to the material's fracture toughness and inversely proportional to the material's modulus and expansion coefficient. Because of silicon nitride's excellent fracture toughness, low expansion rate, and relatively low modulus, silicon nitrides have the highest resistance to crack growth followed by silicon carbide and aluminum oxide.

Localized thermal stresses caused by localized heating anticipated in the wafer seals can also lead to thermal fracture. A parameter measuring the material's resistance to sudden intense heating was calculated for each of the materials and is proportional to the material's strength and thermal diffusivity and inversely proportional to the elastic modulus and expansion coefficient. In order of increasing resistance to intense heating induced fracture of the ceramics included aluminum oxide, silicon carbide, and SN-251 and GN-10 silicon nitrides.

For optimal performance the seal must virtually eliminate leakage. Mounting the relatively low expansion rate ceramic materials in relatively high expansion rate engine panels without seal axial preload raises the possibility of opening small

inter-wafer gaps between the wafers as the seal and panels heat to operating temperature. Using a leakage flow resistance parameter, the effects of relative differences in seal and engine panel expansion coefficients were examined and compared to a minimum flow resistance. Mounting the wafer seal in a relatively high expansion rate engine material (e.g., HS-188) only the aluminum oxide ceramic met the minimum leakage flow resistance, with the other ceramics about 33 percent below the minimum. However, mounting the wafers in a relatively low expansion rate engine material (e.g., Incoloy 909) comparable to several of the engine materials under consideration, the calculated flow resistance was considerably above the minimum for all of the ceramics considered.

Based on these findings the following results were obtained:

1. To exploit the excellent thermal properties of the sintered-alpha silicon carbide material, improvements must be made in producing near-inclusion-free, fracture tough wafers.

2. The superior strength, toughness and moderate thermal properties of advanced silicon nitride ceramics such as SN-251 show great promise for application as hypersonic engine seals if mated with low to moderate expansion rate engine materials.

REFERENCES

1. Steinetz, B.M.; DellaCorte, C.; Sirocky, P.J.: On The Development of Hypersonic Engine Seals. NASA TP-2854, 1988.

2. Steinetz, B.M.: A Test Fixture for Measuring High-Temperature Hypersonic-Engine Seal Performance. NASA TM-103658, 1990.

3. Steinetz, B.M.: High Temperature Performance Evaluation of a Hypersonic Engine Ceramic Wafer Seal. NASA TM-103737, 1991.

4. Tong, M.; and Steinetz, B.M.: Thermal and Structural Assessments of a Ceramic Wafer Seal in Hypersonic Engines. NASA TM-103651, 1990.

5. Richerson, D.W.: Modern Ceramic Engineering. Marcel Dekker, 1982.

6. Hecht, N.: Mechanical Properties Characterization of High Performance Ceramic. Published in, Proceedings of the 27th Automotive Technology Development Contractors Coordination Meeting, SAE, 1990. (Also to be published in Ceram. Eng. Sci. Proc., no. 7-8, 1991.)

7. Weibull, W.: A Statistical Distribution Function of Wide Applicability. J. Appl. Mech., vol. 18, no. 3, Sept. 1951, pp. 293-297.

8. Hasselman, D.P.H.: Thermal Stress Resistance Parameters for Brittle Refractory Ceramics: A Compendium. Am. Ceram. Soc. Bull., vol. 49, no. 12, Dec. 1970, pp. 1033-1037.

9. Chandler, W.T.: Hydrogen-Environment Embrittlement and its Control in High Pressure Hydrogen/Oxygen Rocket Engines. Advanced Earth-to-Orbit Propulsion Technology 1986, vol. 2, R.J. Richmond and S.T. Wu, eds., NASA CP-2437-VOL-2, 1986, pp. 618-634.

10. Incoloy 909 Product Catalog, Publication No. IAI-18, Inco Alloys International, Inc., 1987.

11. Sliney, H.E.; and DellaCorte, C.: A New Test Machine for Measuring Friction and Wear in Controlled Atmospheres to 1200 °C. NASA TM-102405, 1989.

12. Steinetz, B.M.; DellaCorte, C.; and Tong, M.: Seal Concept and Material Performance Evaluation for the NASP Engine. NASA CP-7045, Vol. VI, Structures, 1989, pp. 39-58.

13. Herbell, T.P., et al.: Effect of Hydrogen on the Strength and Microstructure of Selected Ceramics. NASA TM-103674, 1990.

14. Manson, S.S.: Inconel 718. Aerospace Metals Handbook, Article 4103, 1974.

TABLE I. - COMPARISON OF MONOLITHIC CERAMIC PROPERTIES

Property	Temperature	Al_2O_3 99%pure[7]	SiC SA[10]	Si_3N_4 GN-10[12]	Si_3N_4 SN-220[6]	Si_3N_4 SN-251[8]
Mechanical properties:						
Poisson's ratio	R.T.	0.30[7]	0.14[10]	0.27[12]	0.28[6]	0.27[13]
Modulus of elasticity, Msi	R.T.	54[7]	62[2]	44[12]	43[6]	43
	2200 °F	47[7]	58[2]	41	NA	41[14]
4 Point flexural strength, ksi air environment	R.T.	50[7]	58[2]	107[11]	86[6]	94[1]
	2200 °F	40	58[2]	87[11]	44[6]	73[1]
4 Point flexural strength, ksi at R.T. after 100 hrs H_2 exposure at 2200 °F	R.T. after 2200 °F exposure	40	58[5]	87[5,11]	NA	73
Fracture toughness K_{1C}, ksi$\sqrt{in}$	R.T.	3.8[7]	2.7[3,15]	5.1[11]	5.2[6]	6.3[1]
Weibull modulus, m	R.T.	10	5.1[2]	12[12]	11	17[13]
	As noted	NA	11.5[2] 2550 °F	NA	NA	13[13] 2500 °F
Thermal properties:						
Max use temperature, °F	°F	3000	2500	2200	1650	2500
Thermal expansion coefficient, μin./in. °F	RT-2200 °F	4.5[7]	2.2[10]	1.7[12]	1.8[6]	1.7[13]
Thermal conductivity, Btu/h-ft-°F	R.T.	16[7]	73[10]	25[12]	12[6]	37[1]
	2200 °F	3.9[7]	20[9]	11[12]	7[6]	12[13]
Specific heat, Btu/lb °F	R.T.	0.18[7]	0.17[9]	0.14[12]	0.16[6]	0.15[13]
	2200 °F	0.31[7]	0.31[9]	0.30[12]	NA	0.30[4]
Material properties:						
Material density, lb/in.^{3}	R.T.	0.14[7]	0.11[10]	0.12[11]	0.11[6]	0.12[1]
Seal dry weight, lb/linear ft includes: wafers bellows; Inconel strip	R.T.	0.70	0.61	0.64	0.61	0.64

TABLE I. - Concluded.

[1]Yoshida, M; Kokaji, A; and Kogg, K: Silicon Nitride for Automotive Applications. SAE Paper No 890424, Society of Automotive Engineers, 1989.
[2]Hecht, N.: Mechanical Properties Characterization of High Performance Ceramic. Published in Proceedings of the 27th Automotive Technology Development Contractors Coordination Meeting. (Also to be published in Ceram. Eng. Sci. Proc., no. 7-8, 1991.)
[3]Measured in author's laboratory by Micro-Indentation method Fracture toughness method using Evans calculation method.
[4]Kyocera Corporation Central Research Laboratory Internal Report, Entitled "Properties of SN-260," Table 1.
[5]Herbell, T.P., et al.: Effect of Hydrogen on the Strength and Microstructure of Selected Ceramics. NASA TM-103674, 1990.
[6]Kyocera Engineering Ceramics Catalog Information. Catalog No. 4T8912THA, 1989.
[7]Greenleaf Technical Ceramics 99% Purity Alumina. Greenleaf Technical Ceramics Product Catalog Information, Hayward, CA, 94545.
[8]Kyocera Corporation Central Research Laboratory Internal Report No. K41-0003.
[9]DOE Report prepared by Garrett AirResearch Manufacturing Co. of America, DOE Report Page 31-3559.
[10]Carborundum Silicon Carbide Hexoloy SA Grade Catalog Form A12025, May, 1985.
[11]Choi, S.R.; and Salem, J.A.: Strength Toughness and R-Curve Behavior of SiC Whisker Reinforced Composite Si_3N_4 with Reference to Monolithic Si_3N_4. Submitted to Journal of Materials Science, 1991.
[12]Garrett Ceramic Components GN-10 Product Catalog, SPLA-1086A, Torrance, CA, 90509, 1990.
[13]Salem, J.A., et al.: Reliability Analysis of a Structural Ceramic Combustion Chamber. NASA TM-103264, 1990.
[14]Kyocera Corporation Central Research Laboratory Internal Report, Entitled "Typical Properties of SN-251 and SN-252."
[15]Dannels, C.M.; and Dutta, S.: Effect of Processing on Fracture Toughness of Silicon Carbide as Determined by Vickers Indentations. NASA TM-101456, 1989.

TABLE 2. - CERAMIC AVERAGE FRICTION COEFFICIENTS

Sliding condition	Temperature	Silicon carbide	Silicone nitride	Aluminum oxide
Slid against self	R.T.	0.53	0.70	0.88
	1650 °F	0.65	0.80	1.0
Slid against Inconel X-750	R.T.	0.70	NA	0.5
	1650 °F	0.35	NA	0.3

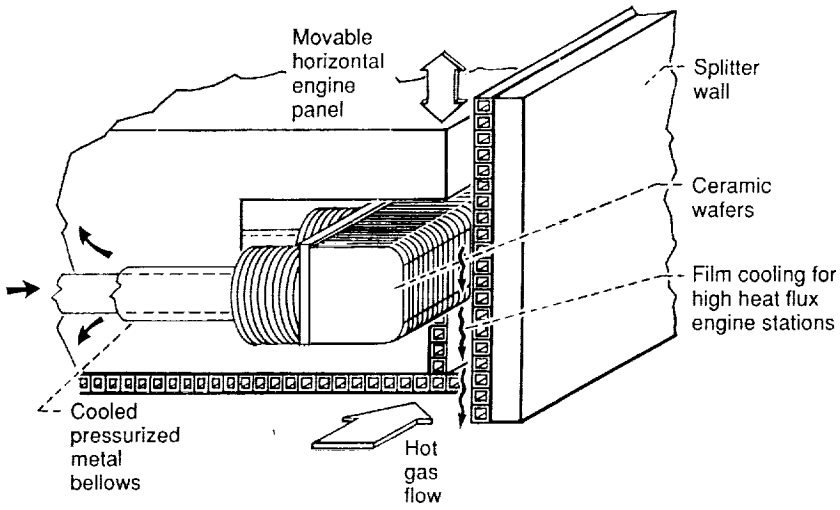

Figure 1.—Isometric of the ceramic wafer seal installed in the movable engine panel.

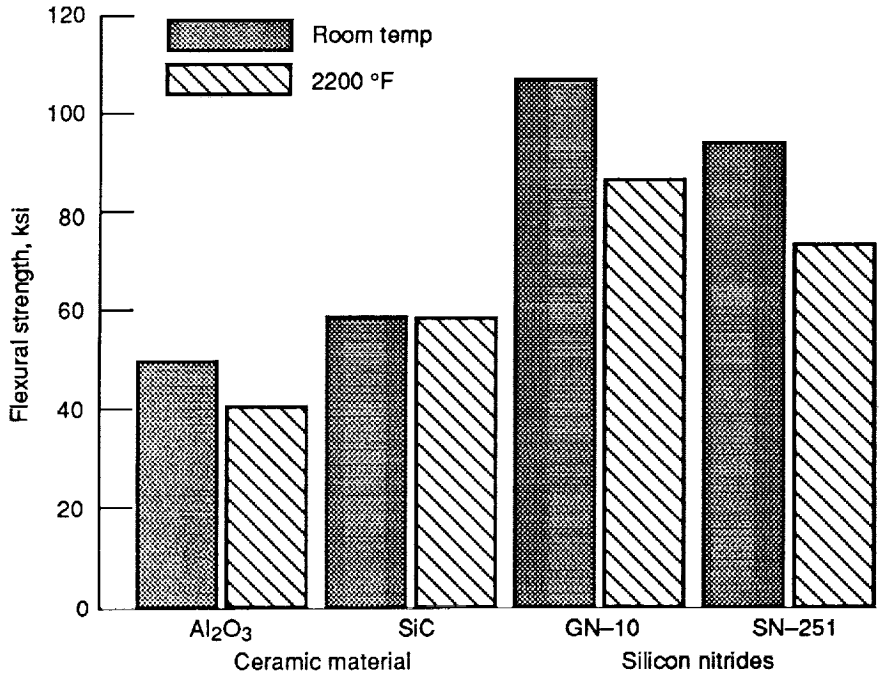

Figure 2.—Flexural strengths (four-point bend) of selected ceramics at room temperature and 2200 °F.

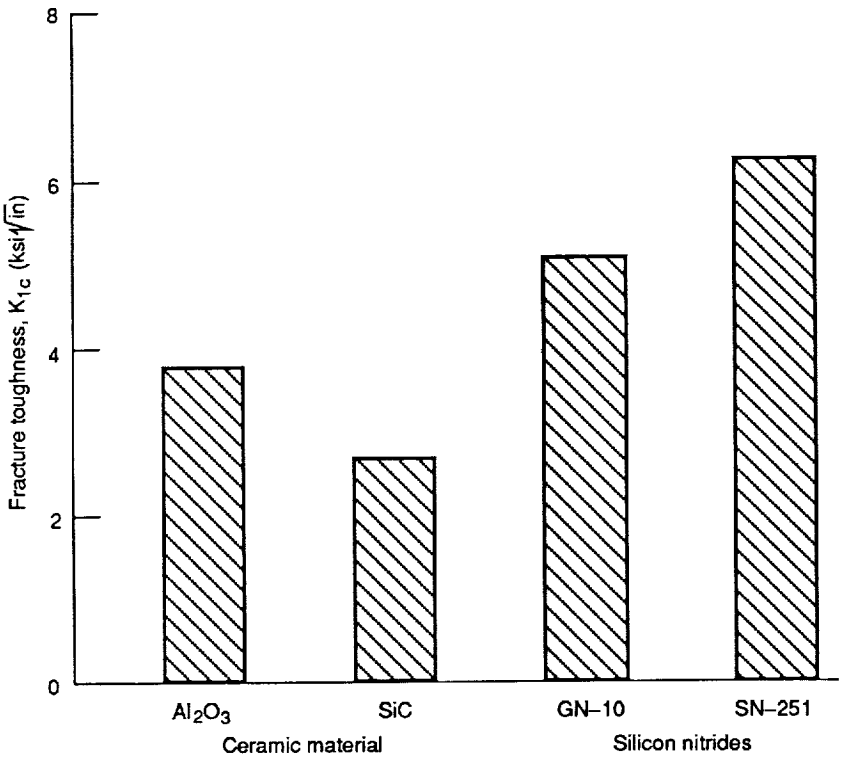

Figure 3.—Ceramic material room temperature fracture toughness.

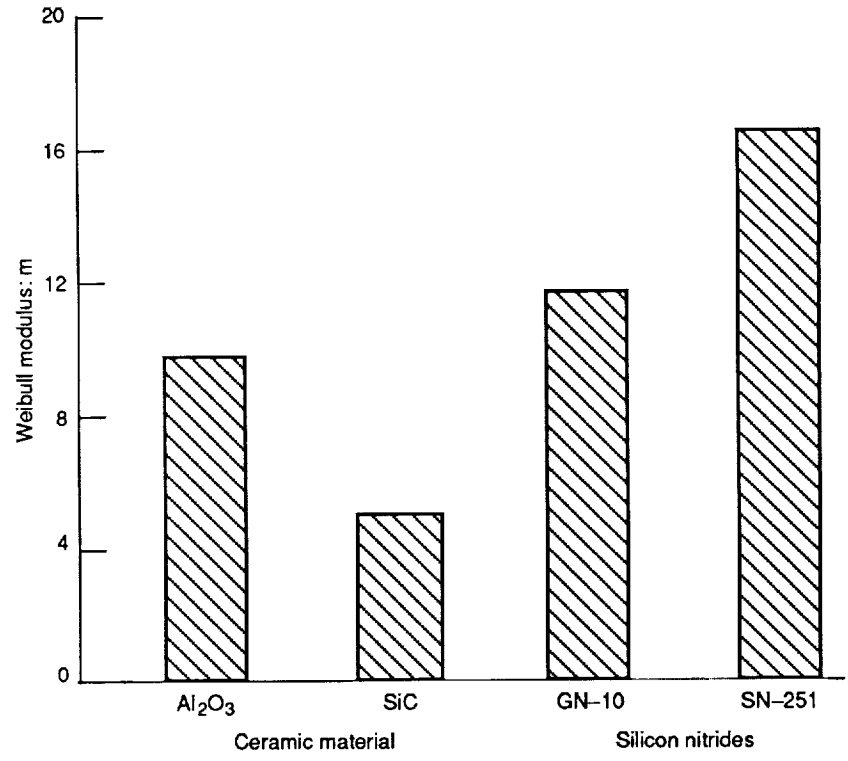

Figure 4.—Ceramic material room temperature Weibull modulus.

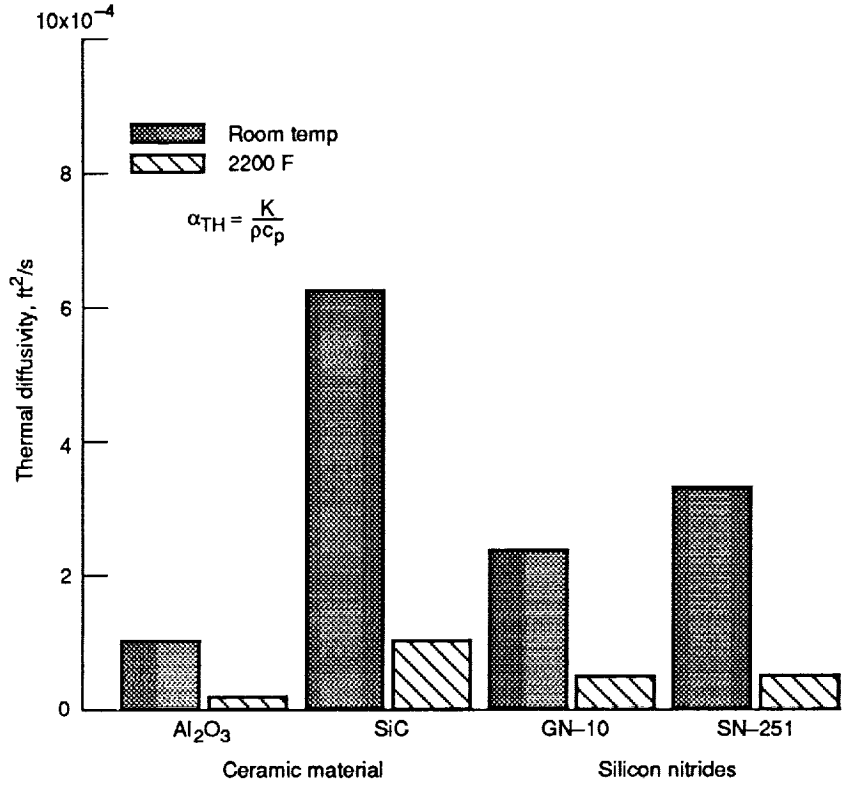

Figure 5.—Thermal diffusivities of selected ceramic materials at room temperature and 2200 °F.

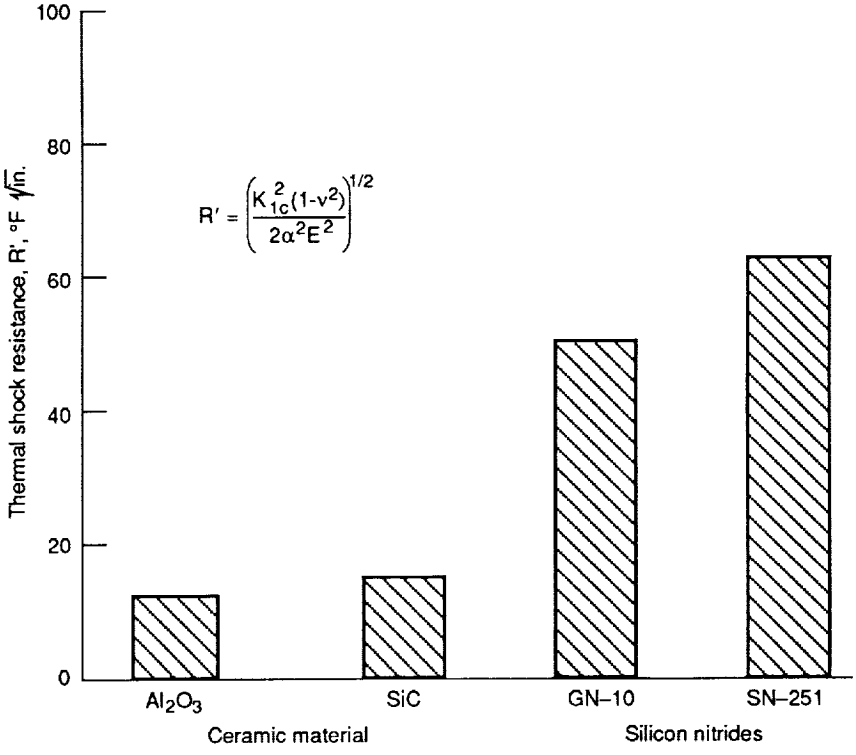

Figure 6.—Material resistance to thermal shock induced crack growth.

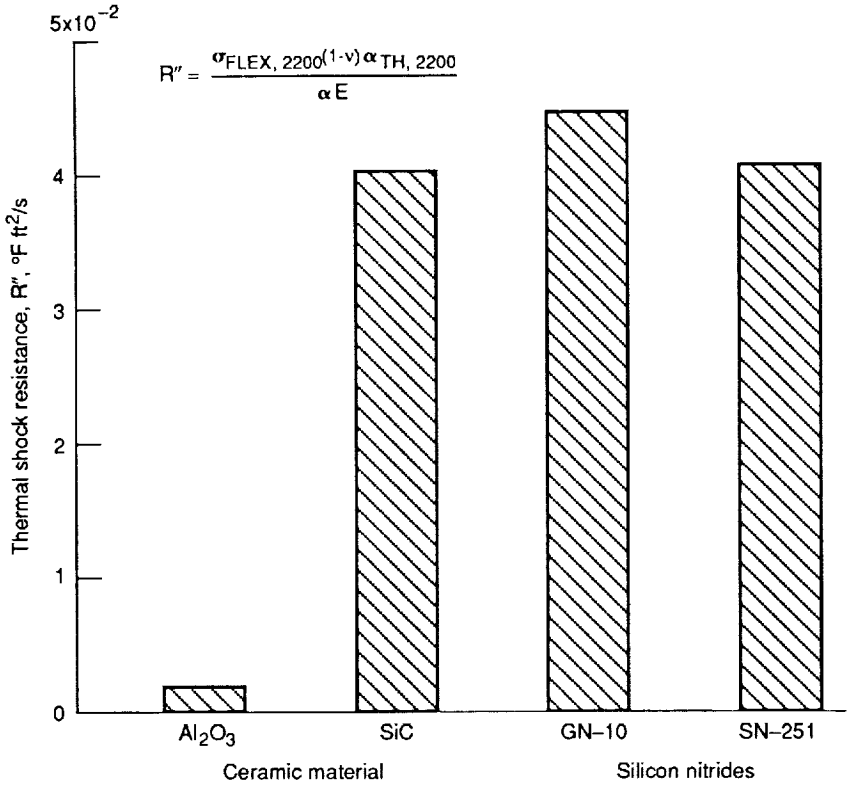

Figure 7.—Material resistance to high surface heating rates.

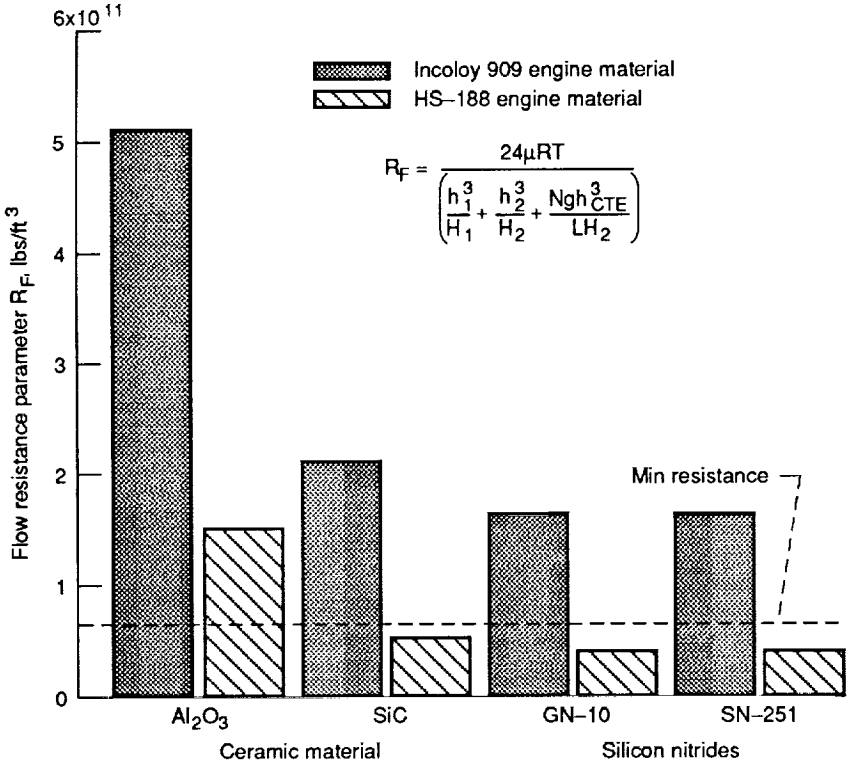

Figure 8.—Seal flow resistance parameter for each of the ceramic materials "mounted" in either a high expansion rate (HS–188) or low expansion rate (Incoloy 909) engine panel material.

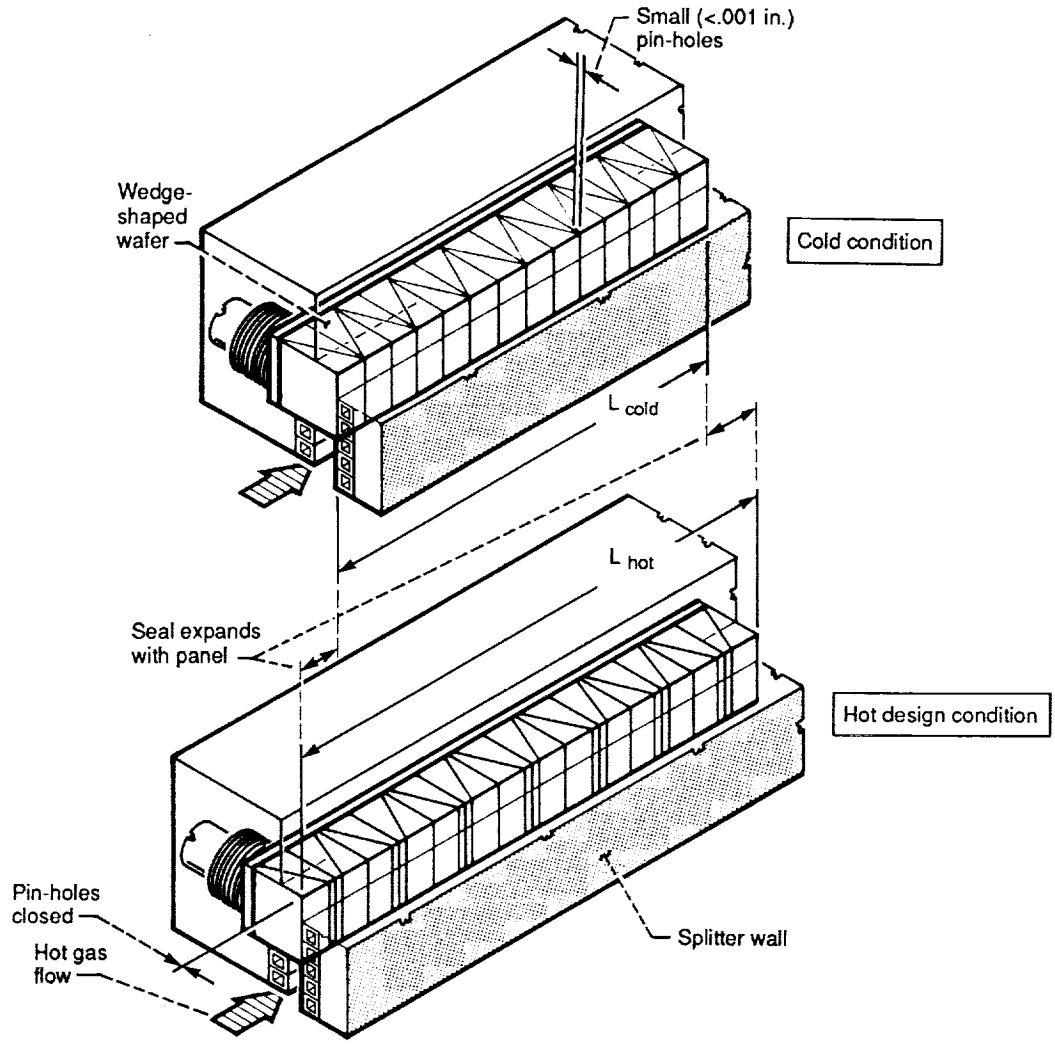

Figure 9.—Wedge-shape wafer concept to overcome mismatch in axial thermal expansion rates of the wafer seal and engine materials.

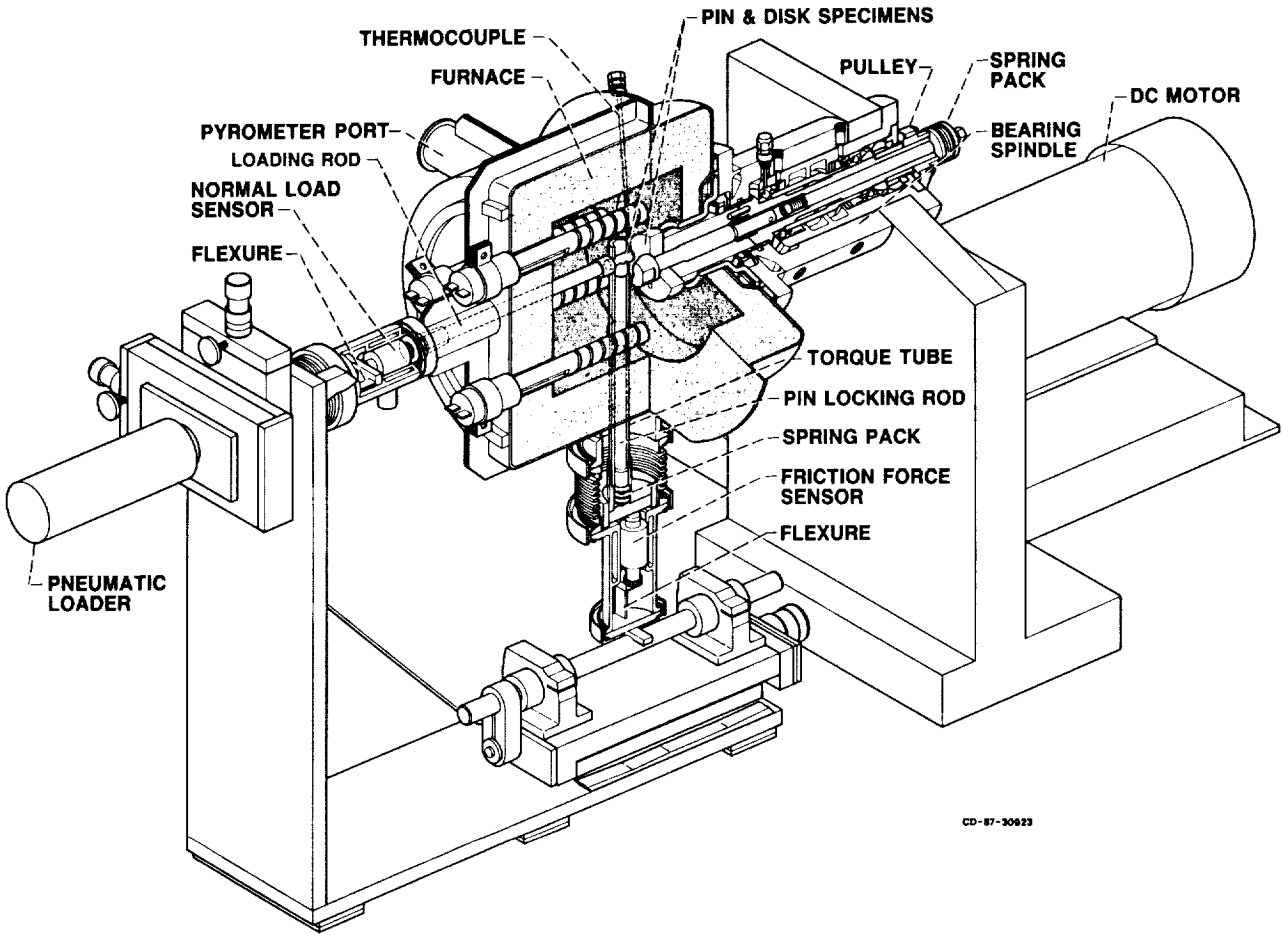

Figure 10.—High temperature pin-on-disk tribometer for measuring seal material friction coefficients at temperature.

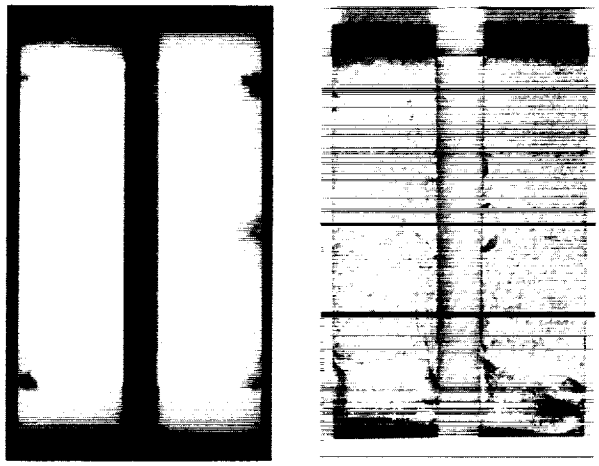

(a) Aluminum oxide wafers. (b) Silicon carbide wafers.

Figure 11.—Photograph of ceramic wafer elements: (a) aluminum oxide wafers after high temperature (1350 °F) testing; (b) silicon carbide wafers with chipped corners after room remperature tests.

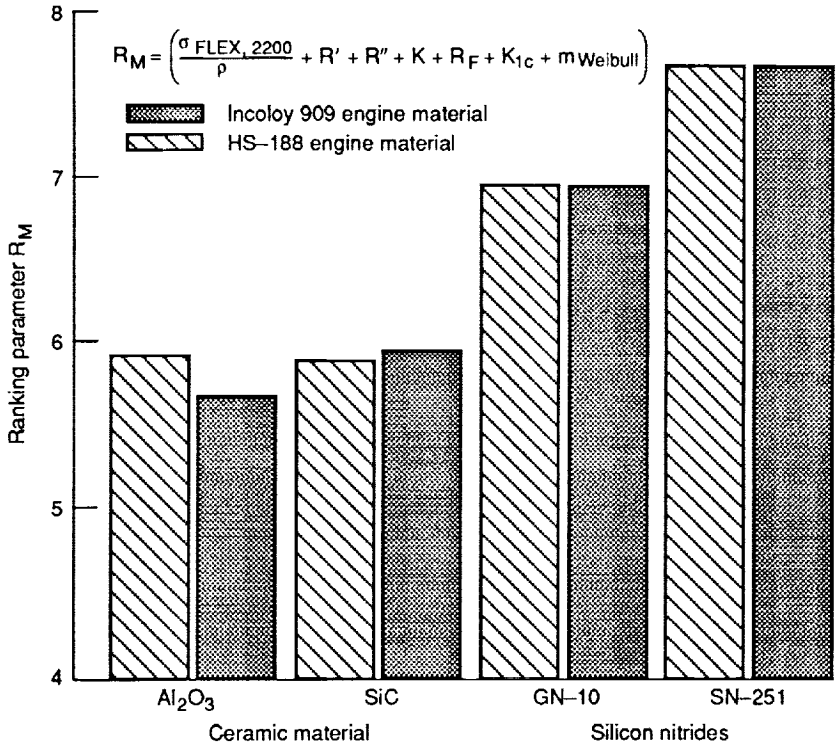

Figure 12.—Ceramic wafer material overall ranking.

NASA
National Aeronautics and Space Administration

Report Documentation Page

1. Report No.	2. Government Accession No.	3. Recipient's Catalog No.
NASA TM - 103795		

4. Title and Subtitle
Evaluation and Ranking of Candidate Ceramic Wafer Engine Seal Materials

5. Report Date
May 1991

6. Performing Organization Code

7. Author(s)
Bruce M. Steinetz

8. Performing Organization Report No.
E - 6082

10. Work Unit No.
505 - 63 - 5B

9. Performing Organization Name and Address
National Aeronautics and Space Administration
Lewis Research Center
Cleveland, Ohio 44135 - 3191

11. Contract or Grant No.

13. Type of Report and Period Covered
Technical Memorandum

12. Sponsoring Agency Name and Address
National Aeronautics and Space Administration
Washington, D.C. 20546 - 0001

14. Sponsoring Agency Code

15. Supplementary Notes
Responsible person, Bruce M. Steinetz, (216) 433 - 3302.

16. Abstract

Modern engineered ceramics offer high temperature capabilities not found in even the best superalloy metals. The high temperature properties of several selected ceramics including aluminum oxide, silicon carbide and silicon nitride are reviewed as they apply to hypersonic engine seal design. A ranking procedure is employed to objectively differentiate amongst four different monolithic ceramic materials considered, including: a cold-pressed and sintered aluminum oxide; a sintered alpha-phase silicon carbide; a hot-isostatically pressed silicon nitride; and a cold-pressed and sintered silicon nitride. This procedure is used to narrow the wide range of potential ceramics considered to an acceptable number for future detailed and costly analyses and tests. The materials are numerically scored according to their high temperature flexural strength; high temperature thermal conductivity (providing a measure of the amount of active cooling required); resistance to crack growth; resistance to high heating rates; fracture toughness; Weibull modulus; and finally according to their resistance to leakage flow, where materials having coefficients of thermal expansion closely matching the engine panel material resist leakage flow best. The cold-pressed and sintered material (Kyocera SN-251) ranked the highest in the overall ranking especially when implemented in engine panels made of low expansion rate materials being considered for the engine, including Incoloy and titanium alloys.

17. Key Words (Suggested by Author(s))	18. Distribution Statement
Seals; Design; Ceramics; High temperature; Hypersonics	Unclassified - Unlimited Subject Category 37

19. Security Classif. (of the report)	20. Security Classif. (of this page)	21. No. of pages	22. Price*
Unclassified	Unclassified	26	A03

NASA FORM 1626 OCT 86

*For sale by the National Technical Information Service, Springfield, Virginia 22161